Target mass dependence of photoneutron spectrum for 16.6 MeV photons on medium-heavy mass targets

Toshiya Sanami[1,2*], *Tyuet Kim* Tran[3], *Hiroshito* Yamazaki[1,2], *Toshiro* Itoga[4], *Yoichi* Kirihara[5], *Yoshihito* Namito[1,2], *Yasuhito* Sakaki[1,2], *Shuji* Miyamoto[6], and *Yoshihiro* Asano[1,6]

[1]High energy accelerator research organization (KEK), Tsukuba, Ibaraki 305-0801, Japan
[2]Graduate University for Advanced Science (SOKNEDAI), Shonan Village, Kanagawa 240-0193, Japan
[3]CEA Saclay, 91191 Gif-sur-Yvette Cedex, France
[4]Japan Synchrotron Radiation Research Institute (JASRI), Kouto, Hyogo 679-5198 Japan
[5]Japan Atomic Energy Agency (JAEA), Tokai-mura, Ibaraki 319-1184, Japan
[6]Osaka University, Ibaraki, Osaka 567-0047, Japan

Abstract. We measured neutron energy spectra for the photonuclear reactions of 16.6 MeV linearly polarized photons on Pb, Au, Sn, Cu, Fe and Ti. The spectra for each target show dependence on the target mass, as well as on the angle between the directions of neutron emission and polarization. The components show angular dependence were extracted from the spectra for each target and compare with the excited levels of residual nuclei. Based on the data, we discuss a plan for further experiments to clearly observe the features of the spectra.

1 Introduction

Photonuclear reactions play an important role in the shielding design of electron accelerators with energies exceeding a few tens of MeV. Cross-sections for this reaction were measured until the 1950s, and cross-section data libraries were prepared based on the results and theoretical research.[1,2,3] Using these libraries, shielding designs have been performed not only for high-power but also for medical-use electron accelerators.

In contrast to the cross-section data, few examples exist of measurements for the energy and angular distribution of neutrons emitted from photonuclear reactions. For example, Mutchler et al.[4] measured the neutron energy distribution from bremsstrahlung photons for various targets. Tagliabue et al.[5] and Baker et al.[6] obtained experimental data showing the anisotropy of neutrons by measuring their angular distribution.

Our group has developed a method to measure the energy and angular distribution of emitted neutrons from photonuclear reactions induced by linearly polarized photons that use the laser inverse Compton scattering technique.[7,8,9] We measured the energy and angular distribution of neutrons for six different target metals (Pb, Au, Sn, Cu, Fe, and Ti) at six different laboratory angles.[10] The results indicate that the neutron energy spectra consist of at least two components: one distributed on the relatively low-energy side showing emission from the equilibrium state and the other showing strong dependency on the direction of polarization of the incident photon, which has a relatively high energy.

In this paper, we introduce our experiment, summarize the characteristics of the results for each target, and discuss future experimental plans to clearly see the features of the spectra.

2 Outline of experiment and data analysis

The details of the experiment, data analysis, and results are described in detail in references.[9,10] We present only an outline of the experiment here.

We conducted the experiment at BL01 of the New SUBARU Synchrotron Radiation Facility in Hyogo, Japan. Fig. 1 shows a photograph of the detector setup

Fig. 1. Neutron detector layout in the hutch.

* Corresponding author: toshiya.sanami@kek.jp

used in the experimental hutch. We injected the 16.6 MeV linearly polarized photons generated by inverse Compton back scattering between the 523 nm laser and 976 MeV electron beam into a target located at the center of the hutch. We measured neutrons produced by photonuclear reactions in the target by using six neutron detectors, five of which were placed on a plane horizontal to the floor at 30°, 60°, 90°, 120°, and 150° with respect to the beam direction. Because the direction of photon polarization was horizontal, the 90° detector on the horizontal plane faced the polarization direction. We placed the other above the target at 90° with respect to the beam direction and polarization. By using the time-of-flight (TOF) method, we determined the neutron energy. For this purpose, we generated the trigger signal of the laser by reducing the accelerator RF signal to control the timing of photon generation. By measuring the time difference between the trigger and detector signals, we derived the TOF distribution of the neutrons. We obtained the energy distribution from the distribution by considering relativistic kinematics.

3 Results and discussions

Fig. 2 shows the results of the Pb target. The left panel shows neutron energy spectra for the horizontal 90° (90), which shows the highest yield, with the vertical 90° (V90) as the lowest among the angles. The right panel shows data points of V90 subtracted from that of 90 as a function of Eγ-Q-En, in which Eγ is the incident photon energy, Q is the Q value of the (γ,n) reaction, and En is the neutron energy. The right panel also includes the level scheme[11] of residual nuclei for the (n, γ) reaction, with a relatively large abundance of target nuclei on the same horizontal scale.

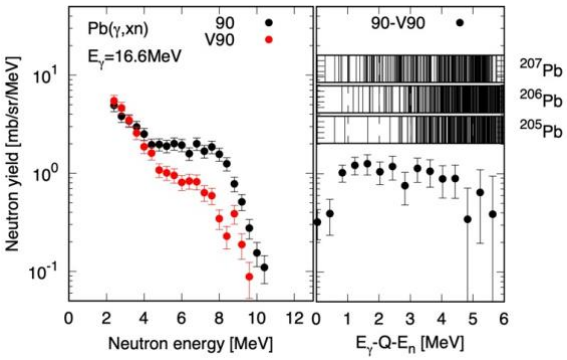

Fig. 2. Experimental results for the Pb target.

The left panel of Fig. 2 shows Pb as a clear polarization-dependent component on its high-energy side. The right panel shows the component with a distribution similar to that of the level scheme and a relatively low neutron yield for the lower Eγ-Q-En side because of the lower number of levels. This could be obvious by performing an experiment with high-energy resolution and isotope enrichment targets. At this time, the energy resolution of the maximum neutron energy reached l0% - larger than the differences in the levels.

Fig. 3 shows the results for the Au target in the same manner as in Fig. 2. The Au target has a mass number similar to that of the Pb target but with fewer polarization-dependent components. In addition, we measured a large number of components corresponding to low excitation levels to reflect dense levels of residual nuclei. Although we describe the value of the (γ,n) cross-section as a function of the mass number, we suggest that the amount of polarization-dependent component cannot be described by this alone.

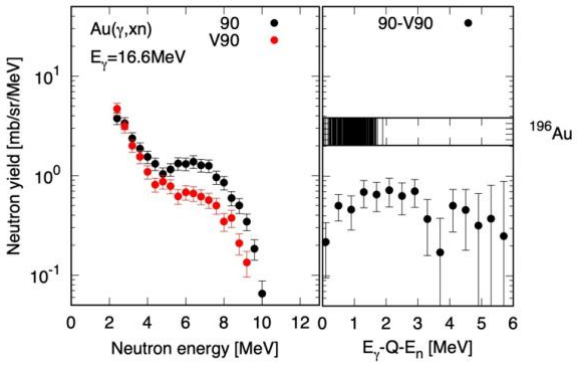

Fig. 3. Experimental results for the Au target.

Fig. 4 shows the results obtained for the tin target. Although the tin target has approximately half the mass of the Au target, the amount of polarization-dependent components compares to that of the Au target. The energy distribution of neutrons reflects a lower number of low-lying levels of residual nuclei, similar to the Pb result.

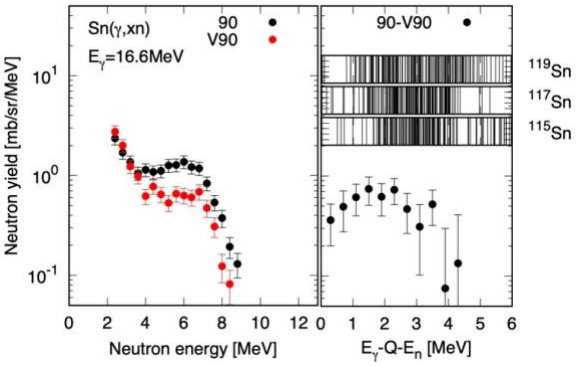

Fig. 4. Experimental results for the Sn target.

Fig. 5 shows the results for the Cu target. The number of polarization-dependent components is lower than that for the previous targets, which is related to the lower incident energy and relatively high Q value. The excited-level structure of the residual nuclei corresponds to the neutron energy distribution - that is, the number of neutrons decreases toward the ground level.

Fig. 6 shows the results for the Fe target. Although the mass number is similar to that of the Cu target, we obtained an even smaller number of polarization-dependent components, reflecting a lower number of low-lying levels of the residual nuclei. Fe is a preferable nucleus to observe neutrons for each low-lying level because of the relatively large energy difference between them.

Fig. 7 shows the results for the Ti target, which showed an angular dependence opposite to that of the

other targets. Thus, the right-side panel shows the V90-90. Seeing this dependence when the incident energy of a photon is increased is quite interesting—that is, when a large number of levels participate in neutron emission. To observe this, an increase of at least 3 MeV is required.

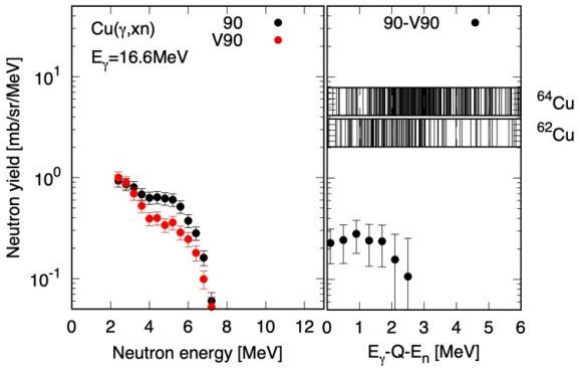

Fig. 5. Experimental results for the Cu target.

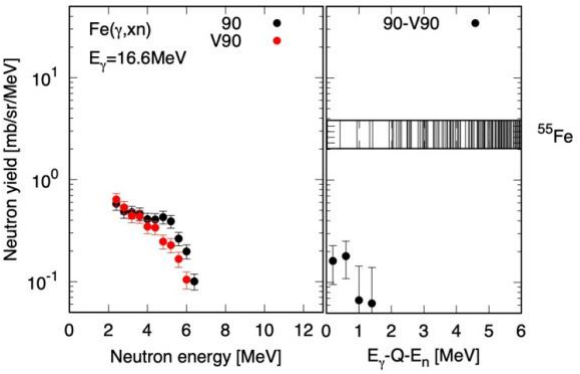

Fig. 6. Experimental results for the Fe target.

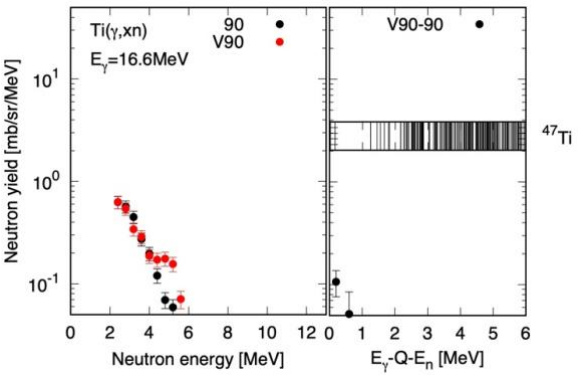

Fig. 7. Experimental results for the Ti target.

4 Conclusions and future work

In this paper, we present experiments on neutron energy spectrum measurements from photoneutron reactions and discuss the characteristics of the results for each target by deducing the energy spectrum of the polarization-dependent component that uses the reference-level scheme of residual nuclei. Based on the above comparison, we suggest several candidates for future experiments. We collected additional data for heavy targets such as Bi, W, and Ta to observe the differences observed for Pb and Au. These are important nuclei for practical applications. Increasing the incident photon energy is also interesting for observing the behavior of Cu, Fe, Ti, and other light nuclei.

Because of the NewSUBARU operation limit, a longer beam time may be required. The most interesting topic of the experiment was improving energy resolution, which require a longer flight path and a shorter detector thickness. Because this causes a low neutron yield, a photon beam intensity enhancement of at least 10 times is required.

Acknowledgements

This work was partially supported by JSPS KAKENHI (grant number 20K12487).

References

1. T. Kawano, Y. S. Cho, P. Dimitriou, D. Filipescu, N. Iwamoto, V. Plujko, X. Tao, H. Utsunomiya, V. Varlamov, R. Xu, R. Capote, I. Gheorghe, O. Gorbachenko, Y.L. Jin, T. Renstrøm, K. Stopani, Y. Tian, G. M. Tveten, J.M. Wang, T. Belgya, R. Firestone, S. Goriely, J. Kopecky, M. Krti ˇcka, R. Schwengner, S. Siem, and M. Wiedeking, arXiv:1908.00471v1.
2. B.L. Berman, "Atlas of photoneutron cross-section obtained with monoenergetic photons," Atomic Data and Nuclear Data Tables, **15**, 319 (1975).
3. H. Utsunomiya, I. Gheorghe, D.M. Filipescu, T. Glodariu, S. Belyshev, K. Stopani, V. Varlamov, B. Ishkhanov, S. Katayama, D. Takenaka, T. Ari-izumi, S. Amano, and S. Miyamoto, Nucl. Inst. Meth. A, **871**, 135 (2017).
4. G.S. Mutchler, Cambridge, Ph.D. thesis, Massachusetts Institute of Technology; 1966.
5. F. Tagliabue and J. Goldemberg, Nucl. Phys., **23**, 144 (1961).
6. R.G. Baker and K. G. McNeill, Can. J. Phys., **39**, 1158 (1961).
7. S. Miyamoto, Y. Asano, S. Amano, D. Li, K. Imasaki, H. Kinugasa, Y. Shoji, T. Takagi, and T. Mochizuki, Radiat. Meas., **41**, S179 (2007).
8. Y. Asano, S. Miyamoto, and LEPS-II collaboration, Prog. Nucl. Sci. Tech., **4**, 252 (2014).
9. Y. Kirihara, H. Nakashima, T. Sanami, Y. Namito, T. Itoga, S. Miyamoto, A. Takemoto, M. Yamaguchi, and Y. Asano, J. Nucl. Sci. Tech. **57**, 444 (2020).
10. T.K. Tuyet, T. Sanami, H. Yamazaki, T. Itoga, A. Takeuchi, Y. Namito, S. Miyamoto, and Y. Asano, Nuclear Inst. and Methods in Physics, A **989** 164965 (2021)
11. ENDSF: Evaluated Nuclear Data Structure File, https://www.nndc.bnl.gov/ensdf/